Research Article | Vol. 11, No. 5 / 1 May 2020 / Biomedical Optics Express 2402
Biomedical Optics EXPRESS

Intraoperative tumor margin assessment using diffuse reflectance spectroscopy: the effect of electrosurgery on tissue discrimination using ex vivo animal tissue models

SARA AZIZIAN AMIRI,[1,*] CARLIJN M. VAN GENT,[1] JENNY DANKELMAN,[1] AND BENNO H. W. HENDRIKS[1,2]

[1]Delft University of Technology, Biomechanical Engineering Department, Delft, The Netherlands
[2]Philips Research, In-Body Systems Department, Eindhoven, The Netherlands
[*]s.azizianamiri@tudelft.nl

Abstract: Using an intraoperative margin assessment technique during breast-conserving surgery (BCS) helps surgeons to decrease the risk of positive margin occurrence. Diffuse reflectance spectroscopy (DRS) has the potential to discriminate healthy breast tissue from cancerous tissue. We investigated the performance of an electrosurgical knife integrated with a DRS on porcine muscle and adipose tissue. Characterization of the formed debris on the optical fibers after electrosurgery revealed that the contamination is mostly burned tissue. Even with contaminated optical fibers, both tissues could still be discriminated with DRS based on fat/water ratio. Therefore, an electrosurgical knife integrated with DRS may be a promising technology to provide the surgeon with real-time guidance during BCS.

1. Introduction

Breast cancer is the most common cancer among women worldwide and the incidence keeps increasing [1]. The standard surgical treatment for early-stage breast cancer patients is breast-conserving surgery (BCS), in which the surgeon aims to remove the tumor while maintaining the natural shape of the breast as much as possible [2]. It has been shown that lack of direct view over the surgical site or surgeon's failure to determine the exact position of the tumor based on preoperative images may lead to incomplete resection of the tumor and incidence of positive margin [3]. Positive margins occur when the excised tumor is not surrounded by at least 2 mm of healthy tissue. The incidence of positive margin during tumor surgery is a widespread problem in clinical practice, but no standard solution has been developed yet [4]. In the case of positive margin detection, re-excision surgery or extra radiation therapy and chemotherapy are required [5–7]. Based on the literature, the occurrence rate for re-excision surgery ranges from less than 10% to around 50% [8].

While positive margin incidence can cause difficulties for patients and hospitals, pre-operative localization of breast lesions, such as needle localization, intraoperative ultrasound, radio-guided surgery, and also intraoperative assessments techniques, such as gross assessment, specimen radiograph, frozen section, and cavity shave margins, seem to be promising techniques to overcome these undesired outcomes [8]. However, all of these techniques have their limitations. For instance, needle localization could be accompanied by affecting incision location, poor cosmetic results, and could be more time consuming while causing more discomfort to the patient [8,9]. Intraoperative ultrasound is an operator-dependent technique requiring extra markers for lesions such as DCIS (Ductal Carcinoma In Situ) [8–10]. In addition to the limitation in detecting small, noncalcified lesions during radio-guided surgery and seed localization, the need to onside nuclear support is associated with consuming more time, costs, and specialist workforce, which is not possible for many facilities [8,11]. Furthermore, the currently available intraoperative

#385621 https://doi.org/10.1364/BOE.385621
Journal © 2020 Received 6 Jan 2020; revised 11 Mar 2020; accepted 1 Apr 2020; published 7 Apr 2020

Biomedical Optics EXPRESS

margin assessment techniques are either not completely reliable in detecting small tumors and DCIS, or can lead to the removal of excess healthy tissue, resulting in undesired cosmetic outputs [8,9]. While applying these techniques decreases the occurrence rate of positive margin during BSC, the occurrence rate remains yet high. Even after the use of the most promising technique still 20% of patients need to go under re-excision surgery, showing that this problem remains unsolved up to now. It seems that for overcoming this challenge emerging technologies need to result in higher diagnostic accuracy in a more cost and time-effective way [12–15].

Recently, researchers proved that Diffuse Reflectance Spectroscopy (DRS) has the potential to be used as a tumor margin assessment technique [12,13,16–25]. Each tissue has its own special intrinsic light absorption and scattering for specific wavelengths which are known as "optical fingerprint". Using DRS in the 400-1600 nm spectral range, De Boer *et al.* showed the Fat/Water ratio is a determinative factor to distinguish malignant tissue from healthy tissue and to determine the exact border of the tumor [16].

Electrosurgery is mostly used during breast-conserving surgery (BCS). With electrosurgery, a high-frequency alternating electrical current is used to cut or coagulate tissue [26]. During this process, high-temperature heat is produced that may cause collateral tissue damage and histological change. These changes can increase the scattering, decrease the depth of photon penetration and alter its optical properties [26–29]. However, recently, Adank *et al*. showed that the DRS system is capable to distinguish muscle tissue from adipose tissue even after cutting or coagulating both tissues using an electrosurgical knife [3]. Based on these results, integrating the DRS system into the electrosurgical knife seems to be a promising approach to provide the surgeon with real-time oncological guidance during cancer surgery. Despite tissue altering during electrosurgery, tissue debris formation is another undesired factor that may affect the DRS measurements. Eschar formation on the electrode of the electrosurgical knife is the most frequent happening, an unwanted event during electrosurgery [26]. Adank *et al*. also mentioned that debris adhering to the optical fibers of the DRS system integrated into the active electrode of an electrosurgical knife is suspected to deteriorate the DRS signal by altering the light behavior and its optical properties.

Therefore, in this research, the characteristics of debris attached to the optical fibers integrated into the electrosurgical knife are investigated, as well as the effect of the type of debris on the DRS signal deterioration and the Fat/Water ratio.

2. Materials and methods

2.1. Sample preparation

To integrate the electrosurgical knife and the DRS system, disposable active blade shape electrodes (Hangzhou Valued Med Tech Co., China), stainless steel tubes (with outer Ø 500 µm and inner Ø 400 µm) and acrylate coated optical fibers (Ø 240 µm) were used. The stainless steel tubes with a length of 1 cm have been welded to the sides of active electrodes as shown in Fig. 1(A), using a laser welding machine. Optical fibers were polished and cleaned to smooth the surface and avoid any roughness. Optical fibers, one connected to the halogen light-source (Avantes, The Netherlands) and one collecting the diffusively reflected light at the surface of the tissue connected to the spectrometer, were placed inside the welded metallic tubes at a 3 mm distance from the center of the emitting fiber to the center of the collecting fiber. Then, the active electrode was placed on the electrosurgical knife.

The optical fibers were connected to a Philips custom-designed diffused reflectance spectroscopy setup (Philips Research, Eindhoven) consisting of a halogen broadband light source (Avantes, The Netherlands) and spectrometers including one spectrometer designated to collect the light in the 400-1000 nm spectral range (Maya2000 Pro, Ocean Optics, USA), and one spectrometer that collects light in the 900-1700nm spectral range (NIRQuest 512, Ocean Optics, USA). The design and application of the diffused reflectance spectroscopy setup have been described in

Biomedical Optics EXPRESS

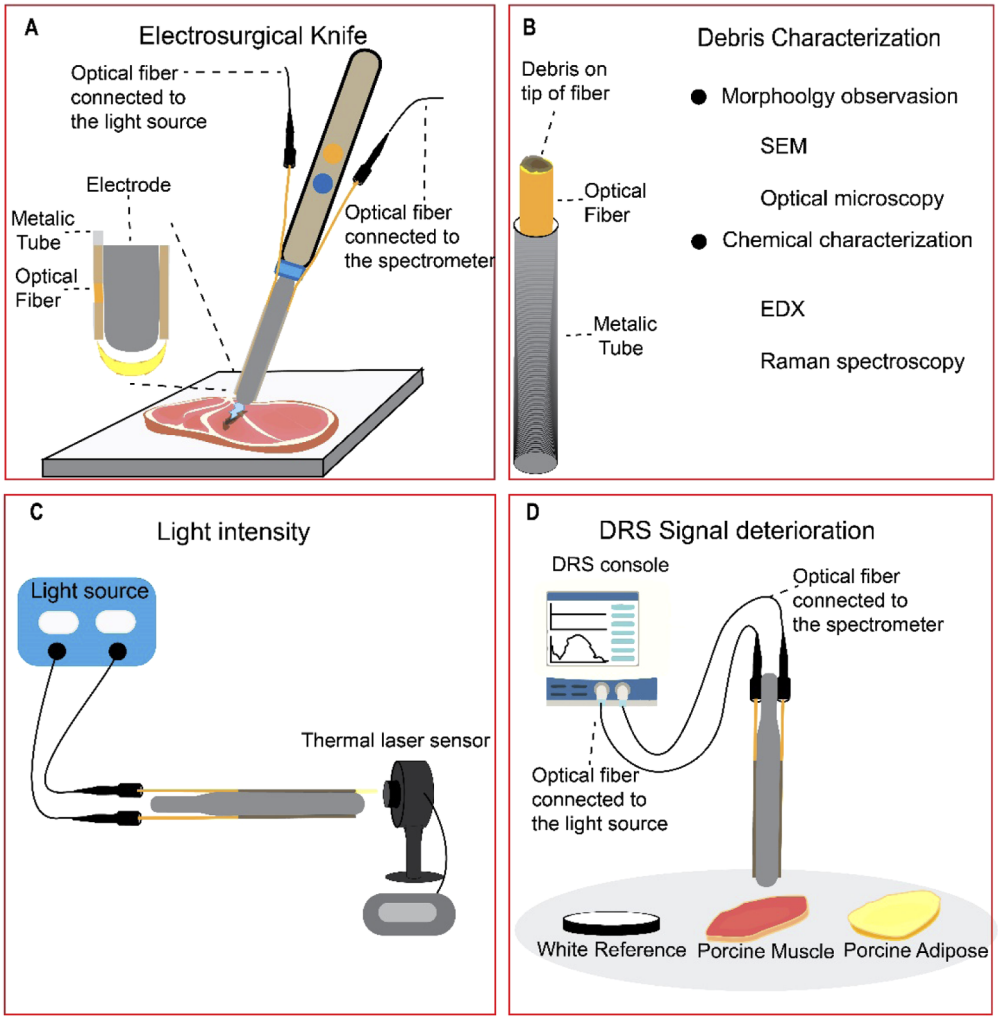

Fig. 1. A) The design of the electrosurgical knife integrated with DRS (fiber-fiber distance = 3 mm). B) Characterizing the debris formed on the tip of optical fibers due to electrosurgery. C) The used setup to measure the intensity of light passing through the clean and used optical fibers. D) The setup to investigate the DRS signal deterioration after electrosurgery with three different sets of optical fiber, Clean Fiber (unused fiber), Muscle Fiber (contaminated with muscle tissue), and Fat Fiber (contaminated with adipose tissue) on three different surfaces (white reference, porcine muscle, and porcine adipose tissue).

Biomedical Optics EXPRESS

more detail in previous publications [3,20,30]. The measured spectra were used as the input for a Philips custom-developed software. The software uses a nonlinear Levenberg–Marquardt inversion algorithm to fit a curve on the measured spectrum and extract the concentration of the chromophore from the fitted data [20].

Before starting the DRS measurements, the system is calibrated to minimize the influence of the ambient light and correcting the system response by placing the tip of the optical fibers at a fixed distance of 2 mm on top of the white reflectance standard,(WS-1-SL, Labsphere Inc., USA). Subsequently, the spectral response of white reference was measured, followed by a background measurement. The DRS system and calibration process applied in this research have been described previously [20,30,31].

As mentioned before by using the Fat/Water ratio of the breast normal tissue (Fat/Water ration>1) and tumor tissue (Fat/Water ration<1), it is possible to distinguish the normal tissue from tumor tissue with high sensitivity and specificity [16]. By considering this, porcine adipose tissue was chosen to simulate the healthy breast tissue as both tissues have a Fat/Water ratio of higher than 1. Also, porcine muscle tissue with a Fat/Water ratio of lower than 1 was selected to simulate the breast tumor tissue which also has a Fat/Water ratio lower than 1. Briefly, similar as in Ref. [3] in all the experiments, the healthy breast tissue and tumor tissue were simulated by porcine adipose tissue and porcine muscle tissue, respectively.

2.2. Debris characterization

To create the samples (contaminated optical fibers) using the electrosurgical knife with integrated DRS, *ex vivo* porcine muscle and adipose tissue, an electrosurgical unit (Valleylab, Medtronic plc, USA) and a dispersive pad were used. The electrosurgical knife was used for 30 seconds, in blend mode combined with a power of 60W, to cut porcine muscle and adipose tissue. For further analysis, the contaminated optical fibers were taken and used for the characterization (Fig. 1(B)). In the text, Clean Fiber, Muscle Fiber, and Fat Fiber refer to the unused optical fiber, the optical fiber contaminated while cutting the porcine muscle tissue, and the optical fiber contaminated while cutting porcine adipose tissue, respectively.

After sample preparation, the used optical fibers (without connectors) were analyzed on morphology by optical microscopy (Keyence VHX-5000, Keyence Corporation, Japan) and scanning electron microscopy (SEM) (JSM-7500F, JEOL Ltd., Japan). For SEM analysis, the optical fibers were coated with a layer of gold using a gold sputter. The samples were placed under both microscopes and different magnifications were used to obtain images of specific parts of interest. The ImageJ software (version 1.52a, National Institutes of Health, USA) [32] was used to measure the diameter of the optical fibers from the images obtained with optical microscopy, before and after use.

To determine the debris chemical composition, the used optical fibers were analyzed on composition by energy-dispersive spectroscopy (EDX) (Noran system SIX, Thermo Scientific, United States). In this technique based on the interaction of a source of X-ray excitation and a sample, the elemental composition of the sample can be investigated [33]. It is suspected that the high temperature produced while working with the electrosurgical knife might cause the melting of the acrylate coating around the core of the optical fiber, which could lead to melted acrylate flowing over the tip of the fiber. To investigate the presence of acrylate traces in the debris formed on the tip of the fibers after use, Raman spectroscopy has been used. A confocal Raman microscope (inVia, Renishaw plc., United Kingdom) with laser light of 752 nm was used to produce the clearest Raman spectrum. First, a spectrum from the acrylate coating was taken and the specific vibration peak related to the acrylate coating was determined. A map of the Raman shift from the entire surface of the optical fiber was made. The whole map was searched for specific vibration peaks corresponding to the acrylate coating determined before. As the

Biomedical Optics EXPRESS

surface of the optical fiber was not smooth due to debris formation, the Raman Spectroscopy was used to search for the acrylate vibration in different layers of the debris.

2.3. Light intensity analysis

In order to quantify the influence of the formed debris on the light transmittance through the optical fiber, the intensity of the light passing through the optical fibers was measured, using a light source (same light source used for DRS measurements) connected to the optical fibers and a high sensitivity thermal laser sensor (NOVA II, Ophir Optronics Solutions, Israel) on the distal side, in front of the optical fiber tip. The light intensity of the optical fibers before and after applying electrosurgery was read from the display of the laser sensor, measured in power (μW), as shown in Fig. 1(C).

2.4. DRS signal deterioration

To measure the effect of electrosurgery on the performance of the optical fibers integrated into the electrosurgical knife, the optical fibers at both sides of the blades were attached to the DRS console as described before, and the signal was recorded. For DRS measurements, three sets of DRS integrated knives were prepared for making each Clean Fiber, Fat Fiber, and Muscle Fiber (three knives to prepare each type of fiber). One of the optical fibers was used as the emitter of light and the other optical fiber was used to collected the light. First, the DRS console was calibrated in the wavelength ranging from 400 to 1600 nm, using clean optical fibers on a white reference (Control group) as described before. With every three sets of each Clean Fiber, Muscle Fiber, and Fat Fiber, three spectra were obtained from white reference, porcine muscle tissue, and porcine adipose tissue separately (three spectra per surface)(Fig. 1(D)). In total nine spectra per optical fiber (Clean Fiber, Muscle Fiber, Fat Fiber) per surface (white reference, muscle tissue, adipose tissue) obtained. In Fig. 5. the average spectrum of these nine spectra with the SD for each type of optical fiber and each surface is shown.

The nine measured spectra were used as the input for a Philips custom-developed software. The software uses a nonlinear Levenberg–Marquardt inversion algorithm to fit a curve on the measured spectra and extract the concentration of the chromophore from the fitted data for each surface and each optical fiber [20]. More information regarding the algorithm used for fitting a curve on the DRS spectrum and calculating the concentration of the chromophores can be found in references [20,31]. The average concentration of the chromophores (± SD) was used to analyze and report the results. The measured optical fit parameters are the amount of blood% (as a percentage of total hemoglobin concentration which is 150 g/liter in normal human blood), scattering at 800 nm, amount of collagen, the total amount of fat and water (fat + water) and the fraction of fat. From the last two parameters, the amount of fat as Fat% and the amount of water as Water% and Fat/Water ratio were calculated [22].

To investigate how the contaminated optical fiber can affect the measurements, for each surface (white reference, muscle tissue, adipose tissue) the statistical analysis performed on the concentration of each chromophore using one-way ANOVA test.

2.5. Statistical analysis

All the experiments were repeated three times. One-way ANOVA was used to investigate whether the samples are significantly different or not. P-values smaller than 0.05 were considered significant.

Biomedical Optics EXPRESS

3. Results

3.1. Debris characterization

The optical fibers used on the tissue (Muscle Fiber and Fat Fiber) became black after being used with an electrosurgical knife (Fig. 2, top Side view row). From the side view of the optical fibers, it can be determined that the head of the optical fiber becomes black with an average length of 0.43 cm for Fat Fiber and 0.9 cm for Muscle Fiber. The diameter of the clean optical fiber obtained from the SEM images is 238.9 ± 1.95 µm with an acrylate coating with 10 µm width on each side. The Muscle Fiber and Fat Fiber diameter changed to 223.7 ± 4.5 and 216.6 ± 9.2 µm, respectively, with a nonsignificant difference between the two fibers ($p = 0.19$).

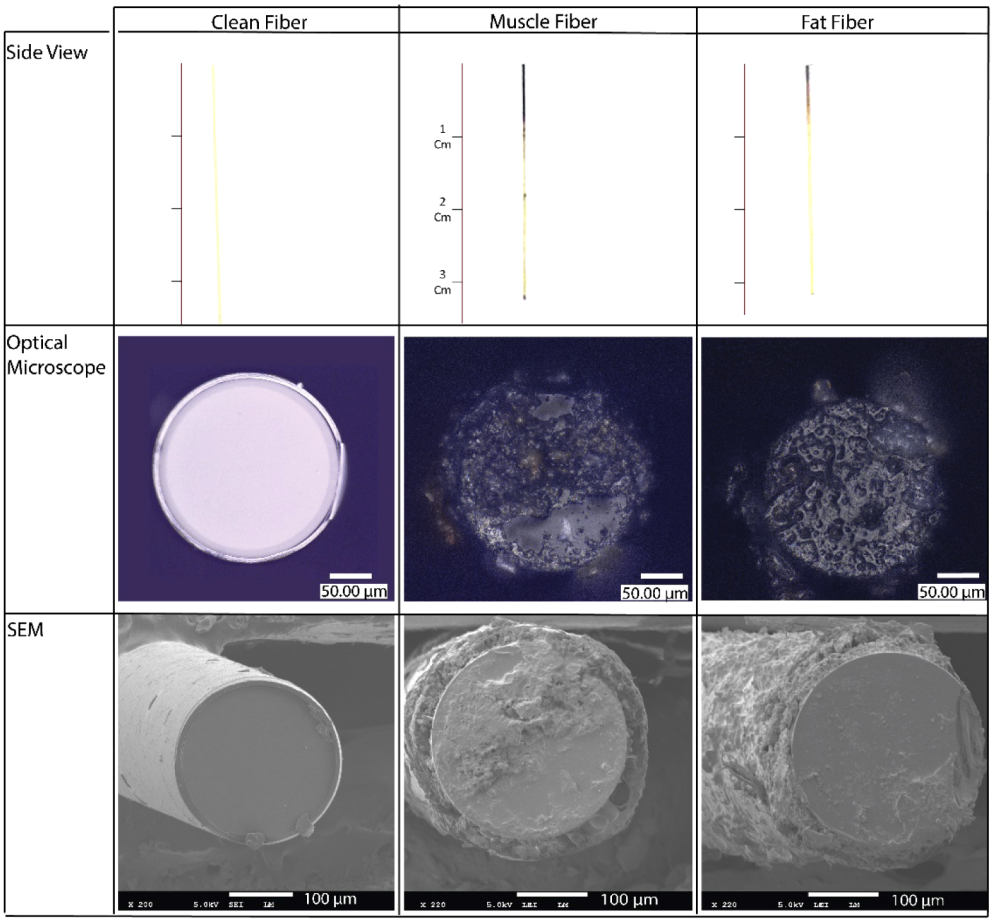

Fig. 2. The shape and morphology of the optical fibers before and after electrosurgery, investigated by optical microscopy (second row) and scanning electron microscopy (SEM, third row).

Meanwhile, based on the optical microscopy and SEM images (Fig. 2), less debris was formed on the tip of Muscle Fiber than Fat Fiber. While cutting porcine muscle tissue with the electrosurgical knife, tissue burning and carbonization was significant. However, after cutting the porcine adipose tissue, there was more melted fat on the optical fiber and surface of the electrode than burned tissue. Also, there were more traces of unburned biological tissue on the electrode and the metallic tubes of the knife used for cutting adipose tissue compared to those used for

Biomedical Optics EXPRESS

cutting muscle tissue. This is also observed for the Fat Fiber, which has some fat like pieces attached to it as shown in Fig. 2.

When using EDX to map the chemical composition it was found that a Clean Fiber consists of a core made of silica or SiO_2 (Si (silicone), in blue color, and O (Oxygen) in green and an Acrylate based coating which contains C (Carbone) shown in red color (Fig. 3, top row). After applying the electrosurgical knife the surface of both contaminated fibers gets red meaning the carbon is covering the optical fibers (Fig. 3, middle and bottom row). The density of the green color (presenting oxygen) and blue cover (presenting Si) decreases, showing that the contamination is covering the surface of the core. For both used optical fibers (Muscle Fiber and Adipose Fiber) there are traces of the Sodium (Na), Magnesium (Mg), Potassium (K) on the top. Furthermore, the EDX of Muscle Fiber confirms the existence of Iron (Fe) on the tip.

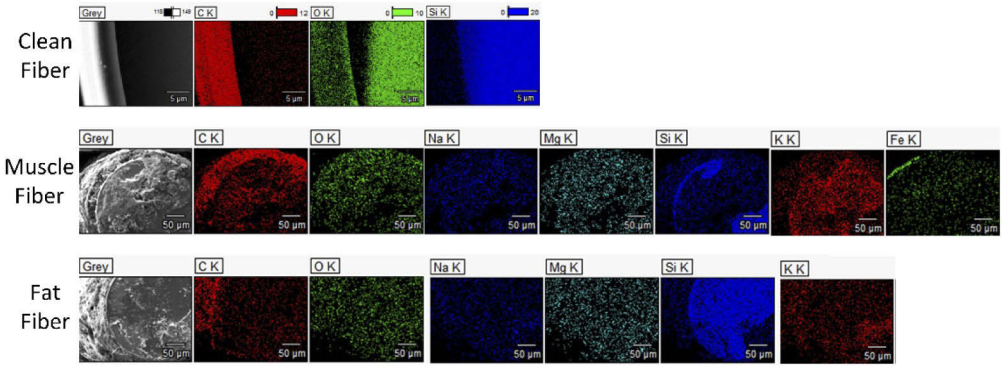

Fig. 3. EDX (energy-dispersive spectroscopy) results taken from the tip of Clean Fiber, Muscle Fiber, and Fat Fiber.

The side view picture of a used optical fiber is shown in Fig. 4(A). Based on this picture, it can be determined that the acrylate coating has vanished for approximately 500 µm from the tip of optical fiber. Raman spectroscopy of the clean optical fibers shows three main peaks, one at 1377, 1618 and 1782 Raman shift (cm^{-1}), respectively (Fig. 4(B)). Next, the Raman map taken from three different layers of the top surface of the Muscle Fiber and Fat Fiber was searched for the peaks found for acrylate coating. However, neither those peaks nor any other specific peak than the common silica glass was found in these three layers of the debris, indicating that vanished acrylate coating did not play a role in debris formation.

3.2. *Light intensity analysis*

The intensity of the light passing through the clean optical fiber and the used optical fibers measured using a light source and laser sensor showed that the average power loss for the Muscle and Fat Fiber is 45.64%±2.9 and 53.44%±19.77, respectively.

3.3. *DRS signal deterioration*

After fitting the spectra using the software, the fitted spectra have been used to make an average spectrum for each Clean Fiber, Muscle Fiber and Fat fiber in front of the white reference, muscle tissue, and adipose tissue which is shown in Fig. 5 along with the SD area.

Spectra obtained using contaminated optical fibers display a decreased intensity on white reference and porcine muscle and adipose tissue for the 400-1600 nm spectral range. Fat Fiber lost more light intensity than Muscle Fiber. The spectrum of both Muscle Fiber and Fat Fiber on the white reference shows the main absorption peaks at wavelengths of 1211, 1393 and 1474 nm.

Biomedical Optics EXPRESS

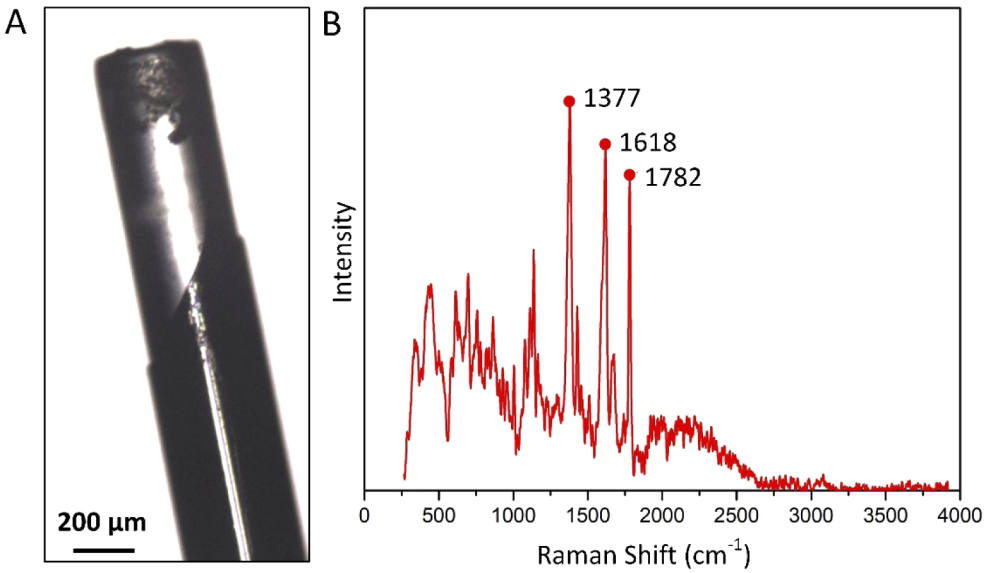

Fig. 4. (A) a side view picture of a used optical fiber integrated into the electrosurgical knife. (B) Raman spectrum is taken from the acrylate coating of clean optical fiber.

The spectra of Muscle Fiber and Fat Fiber on muscle tissue shows similar main peaks compared to Clean Fiber on muscle tissue. For the Fat Fiber, the absorption peak at 500-600 nm related to the blood region is less distinct. For both Muscle Fiber and Fat Fiber the slope of the spectrum between 700-900 nm decreases.

The spectrum obtained from porcine adipose tissue using optical fibers is shown in Fig. 5(C). Again the Fat Fiber spectrum shows a less distinct peak at the 500-600 nm region. Also at wavelengths between 600 to 800 nm, the spectrum of Fat Fibers shows a smaller slope than the spectrum of Muscle and Clean Fibers.

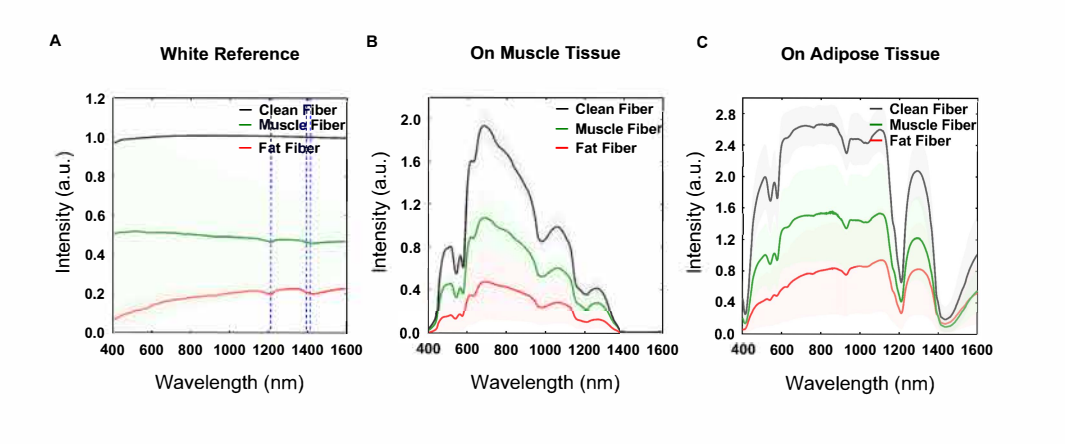

Fig. 5. Fitted spectra using Clean Fiber, Muscle Fiber and Fat fiber in front of the (A) white reference, (B) in contact with muscle tissue and (C) in contact with adipose tissue.

Biomedical Optics EXPRESS

Despite the intensity lost and a few changes, the spectra of the used optical fibers from white reference, porcine muscle, and fat tissue preserve the overall shape found in the spectrum taken by the Clean Fiber on the same tissues.

In Fig. 6. the average of each chromophore concentration ± SD and Fat/Water ratio ± SD is shown. Fat Fiber on the white reference has a Fat% of 3.6% which is significantly different from the Fat% of the Clean Fiber on the white reference. Moreover, the Muscle Fiber shows a very low-Fat % with no significant difference with the control group. However, the Fat% of the spectra of porcine muscle and adipose tissue taken by Fat Fiber and Muscle Fiber is not significantly different from the Fat% of the spectra of the same tissues taken by the Clean Fiber.

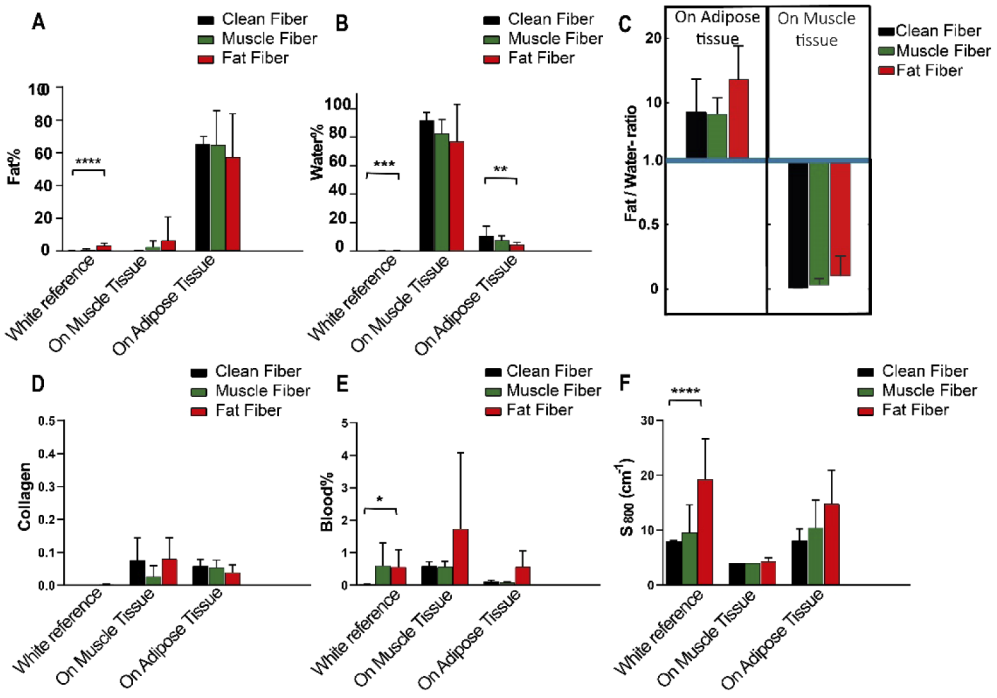

Fig. 6. The concentration of chromophores derived from the obtained spectra using Clean Fiber (black), Muscle Fiber (green) and Fat Fiber (red).

Water% for all the optical fibers on the white reference was negligible. Also, the difference of Water% between the Muscle Fiber and the Clean Fiber on all surfaces was not significant. The Water% between Clean Fiber and Fat Fiber for both white reference and adipose tissue showed a significant difference.

Figure 6(C) shows the Fat/Water ratio for porcine muscle and adipose tissue extracted from the spectra taken by clean and used optical fibers. The Fat/Water ratios for muscle tissue measured using Clean Fiber, Muscle Fiber and Fat Fiber are less than 1. While the Fat/Water-ratio of adipose tissue measured using Clean Fiber, Muscle Fiber and Fat Fiber are more than 1 (around 10).

The amount of Collagen for Muscle Fiber and Fat Fiber on the white reference, muscle, and adipose tissue do not show a significant difference with the amount of Collagen of Clean Fiber on the same surfaces.

Although less than 1% blood on the tip of the Muscle Fiber and Fat Fiber has been detected, the Blood% measured using contaminated optical fibers on muscle and adipose tissue shows no significant difference compared to the measured Blood% of Clean Fiber on same tissues.

Biomedical Optics EXPRESS

Figure 6(F) shows that the reduced scattering (at 800 nm) has increased more for Fat Fiber and less for Muscle Fiber on the white reference. The scattering measured with the Fat Fiber has a significant difference with the scattering measured with the Clean Fiber on the white reference. This increased scattering showed that the contamination on the tip of Fat Fiber can alter the scattering. The difference of reduced scattering at 800 nm between Clean Fiber, Muscle Fiber and Fat Fiber is not significant for the spectra obtained from the muscle and adipose tissue.

4. Discussion

In this study, we investigated the possibility of integrating a DRS system into the electrosurgical knife to investigate whether it would be possible to provide the surgeon with an intraoperative tumor margin assessment. The focus of this research was on the effect of the electrosurgery on the performance of the DRS system.

4.1. Debris characterization

The results of debris characterization show that electrosurgery alters the shape and morphology of the optical fibers, integrated onto the electrode of the electrosurgical knife. During electrosurgery, the temperature around the electrodes significantly increases due to the passing electric current through the tissue [34]. By leading this current through the tissue, the temperature rises to 100-400 °C and when temperature excess 200 °C, carbonization occurs and tissue turns black [35]. Furthermore, results from the diameter measurement of the tip of optical fibers indicate that the diameter of the optical fibers decreased with 20 µm which is almost equal to the width of the Acrylate coating around the core of the optical fiber. This means that after using the optical fibers with the electrosurgical knife, the acrylate coating around the optical fiber vanished. The results of the Raman spectroscopy of acrylate coating and the contamination shows that there is no trace of melted acrylate coating on different layers of the debris, indicating that the acrylate coating has nothing to do with the debris formation on the tip. Another possibility can be that the acrylate coating melts and vaporizes during the use of the electrosurgical knife or that it attaches to the wall of the stainless steel tube.

The black appearance of the head of the optical fibers can be due to the carbonization of the tissue close to it exposed to high-temperature heat and also some unburdened biological tissue. At temperature around 200°C, carbonization occurs, in which the organic molecules will break and carbon molecules with a brown and black appearance will appear [26,35]. Meanwhile, the traces of the Na, Mg, and K confirm that some biological tissue residuals, as well as carbonized tissue, are covering the surface of the used optical fibers. Furthermore, on the Muscle Fiber, a trace of Fe is found, which is a building component of blood [36].

The average length of the burned area of the optical fibers used for cutting porcine muscle is longer than the average length of the burned area of the optical fibers used for cutting the porcine adipose tissue. The thermal conductivity of the porcine muscle (11×10^{-4} cal/cm sec °C) is around 3 times higher than the thermal conductivity of the porcine adipose tissue (3.8×10^{-4} cal/cm sec °C) [35]. So in comparison with muscle tissue, adipose tissue acts as a heat insulator and guards the blade and optical fibers from excessive heat and burning.

Meanwhile, the SEM shows more distinct debris particles attached to the tip of Fat Fiber than Muscle Fiber. As mentioned above, the heat insulation nature of fat may lead to less burned tissue. The lower burning effect produces less burned tissue while producing more isolated and clingy fat pieces with a tendency to attach to the optical fiber tip. While the burned debris is smaller in size, the clingy and isolated fat residues are bigger and cover more surface, which is visible also in the SEM and optical microscopy pictures. This can cause less light passing through the Fat Fiber than Muscle Fiber and Clean Fiber.

Biomedical Optics EXPRESS

4.2. DRS signal deterioration

The DRS spectrum obtained by used optical fibers on white reference shows three main absorption peaks at 1211 nm, 1393 nm, and 1414 nm, which are exactly the absorption peaks of Lipid [37]. This indicates that the main substrate on the tip of Muscle Fiber and Fat Fiber is the lipid, which is in agreement with the results of EDX. Although the intensity of the spectrum obtained using Muscle and Fat Fiber on porcine muscle and adipose tissue decreases, the overall shape of the DRS spectrum remains the same as the spectrum of the Clean Fiber used on the same tissues.

The Fat/Water ratio for adipose tissue, simulating the breast normal tissue, measured using used optical fibers remains greater than 1, whereas, the Fat/Water ratio for the muscle tissue simulating the breast tumor tissue remained lower than 1. This indicates that regarding the results of de Boer *et al*. [16], the integrated DRS system of the electrosurgical knife has the potential to distinguish the muscle tissue from adipose tissue based on Fat/Water ratio, even when the measurements are performed by the used and contaminated optical fibers. Photons between the emitter and collector fiber travel in a "banana-shaped" trajectory inside the tissue (Fig. 1(A)). It has been shown that the depth of this banana-shaped region, is approximate of the order of the fiber distance [38,39]. Accordingly, we expect that as far as the contamination on the tip of the optical fibers is only a thin layer of debris without any strong absorbing (in wavelength 400 nm to 1600 nm) component, it will not be affecting the results of DRS significantly. The effect of such a thin layer on the DRS outputs is negligible compared to the effect of the larger tissue volume, through which the light travels. Meanwhile, the results of the experiments also confirm that the thin layer of debris formed during the use of the electrosurgical knife does not have a significant effect on the results of DRS and its tissue discrimination capability.

During cutting different tissues with the DRS integrated electrosurgical knife, sometimes the produced debris due to electrosurgery, stuck in the empty gap between the optical fiber and inner wall of the metallic tube. Despite the weak connection, sometimes these pieces of the debris are big in size and may cover the area around the tip of optical fiber and don't let the light pass. To avoid these to happen, the void gap between the optical fiber and metallic tube should be confined. Solutions might be reducing the size of the metallic tube or filling this void with a filler material.

Moreover, in our *ex vivo* experiments, the blood perfusion is missing. It has been shown that the presence of blood and methemoglobin (a blood derivative upon coagulation), would only influence the visible region of the spectrum and therefore would not affect the Fat/Water ratio [40]. However, in *in vivo,* the high volume of the blood in contact with the electrosurgical knife can lead to producing more debris as well as a thicker layer of the contamination resulting in more light intensity loss. To minimize the effect of the contamination, the optical fiber can be protected by a transparent material. A transparent material with self-cleaning properties can protect the tip of the optical fiber from being in direct contact with the tissue while maintaining the surface, which is in front of the optical fiber, clear due to the inherent ability of the material to remove the debris. Hence, developing a new design for integrating the optical fiber to the electrosurgical knife to have the minimum contamination and meanwhile be as close as possible to the tip of the electrode of the electrosurgical knife (to provide the connection between optical fibers and the exposed tissue), is something that should be considered for further developing the electrosurgical knife.

5. Conclusion

In this study, we investigated the effect of electrosurgery on the performance of the diffused reflectance spectroscopy system integrated into the tip of the electrosurgical knife. Debris formed on the tip of optical fibers is made of carbonized and unburned tissue. Although the light intensity of the DR spectra decreased after electrosurgery, the overall shape of the spectra remains significantly the same for each tissue. Furthermore, there was no significant difference between the concentration of the chromophores of the tissues measured by clean optical fibers and used

Biomedical Optics EXPRESS

optical fibers. Also, the Fat/Water ratio, which is the determinant parameter in distinguishing breast normal tissue (Fat/Water ratio>1) from breast tumor tissue (Fat/Water ratio<1), measured from the spectra taken by used fibers for muscle tissue remained lower than 1 and for adipose tissue remained greater than 1. This shows that the electrosurgery does not affect the performance of the diffused reflectance spectroscopy integrated on the electrosurgical knife, and the system still can distinguish normal tissue from tumor tissue despite the effects of electrosurgery. Hence, this novel electrosurgical knife with integrated diffused reflectance spectroscopy technology may provide the surgeon with real-time oncological guidance during breast-conserving surgery with the ultimate goal of reducing the positive margin incidence.

Funding

The Netherlands Organization for Health Research and Development (ZonMw) (104006002).

Disclosures

None of the authors who are affiliated with the Delft University of Technology (S.A. and J.D,) have financial interests in the subject matter, materials, or equipment or with any competing materials and did not receive any payments from Philips. The author affiliated with Philips Research (B.H.W.H.) has financial interests in the subject matter, materials, and equipment, in the sense that he is an employee of Philips. The prototype system described in this article is currently a research prototype and is not for commercial use.

References

1. E. R. Sauter, "Breast cancer prevention: Current approaches and future directions," Eur J Breast Health **14**(2), 64 (2018).
2. C. Chiappa, F. Rovera, A. D. Corben, A. Fachinetti, V. De Berardinis, V. Marchionini, S. Rausei, L. Boni, G. Dionigi, and R. Dionigi, "Surgical margins in breast conservation," Int. J. Surg. **11**, S69–S72 (2013).
3. M. W. Adank, J. C. Fleischer, J. Dankelman, and B. H. Hendriks, "Real-time oncological guidance using diffuse reflectance spectroscopy in electrosurgery: the effect of coagulation on tissue discrimination," J. Biomed. Opt. **23**(11), 1 (2018).
4. C. M. O'Kelly Priddy, V. A. Forte, and J. E. Lang, "The importance of surgical margins in breast cancer," J. Surg. Oncol. **113**(3), 256–263 (2016).
5. E. Sadot, B. G. Koerkamp, J. N. Leal, J. Shia, M. Gonen, P. J. Allen, R. P. DeMatteo, T. P. Kingham, N. Kemeny, and L. H. Blumgart, "Resection margin and survival in 2368 patients undergoing hepatic resection for metastatic colorectal cancer: surgical technique or biologic surrogate?" Ann. Surg. **262**(3), 476–485 (2015).
6. M. S. Moran, S. J. Schnitt, A. E. Giuliano, J. R. Harris, S. A. Khan, J. Horton, S. Klimberg, M. Chavez-MacGregor, G. Freedman, and N. Houssami, "Society of Surgical Oncology–American Society for Radiation Oncology consensus guideline on margins for breast-conserving surgery with whole-breast irradiation in stages I and II invasive breast cancer," Ann. Surg. Oncol. **21**(3), 704–716 (2014).
7. M. Pilewskie and M. Morrow, "Extent and role of margin control for DCIS managed by breast-conserving surgery," in *Ductal Carcinoma In Situ and Microinvasive/Borderline Breast Cancer* (Springer, 2015), pp. 67–83.
8. C. Reyna and S. M. DeSnyder, "Intraoperative margin assessment in breast cancer management," Surg Oncol Clin N Am **27**(1), 155–165 (2018).
9. R. G. Pleijhuis, M. Graafland, J. de Vries, J. Bart, J. S. de Jong, and G. M. van Dam, "Obtaining adequate surgical margins in breast-conserving therapy for patients with early-stage breast cancer: current modalities and future directions," Ann. Surg. Oncol. **16**(10), 2717–2730 (2009).
10. R. L. Klein, J. A. Mook, D. M. Euhus, R. Rao, R. T. Wynn, A. B. Eastman, and A. M. Leitch, "Evaluation of a hydrogel based breast biopsy marker (HydroMARK®) as an alternative to wire and radioactive seed localization for non-palpable breast lesions," J. Surg. Oncol. **105**(6), 591–594 (2012).
11. R. Rao, A. Moldrem, V. Sarode, J. White, M. Amen, M. Rao, V. Andrews, D. Euhus, L. Radford, and M. Ulissey, "Experience with seed localization for nonpalpable breast lesions in a public health care system," Ann Surg Oncol **17**(12), 3241–3246 (2010).
12. A. Keller, P. Bialecki, T. J. Wilhelm, and M. K. Vetter, "Diffuse reflectance spectroscopy of human liver tumor specimens-towards a tissue differentiating optical biopsy needle using light emitting diodes," Biomed. Opt. Express **9**(3), 1069–1081 (2018).
13. B. S. Nichols, C. E. Schindler, J. Q. Brown, L. G. Wilke, C. S. Mulvey, M. S. Krieger, J. Gallagher, J. Geradts, R. A. Greenup, and J. A. Von Windheim, "A quantitative diffuse reflectance imaging (QDRI) system for comprehensive surveillance of the morphological landscape in breast tumor margins," PLoS One **10**, e0127525 (2015).

Biomedical Optics EXPRESS

14. L. Jacobs, "Positive margins: the challenge continues for breast surgeons," Ann. Surg. Oncol. **15**(5), 1271–1272 (2008).
15. E. R. St John, R. Al-Khudairi, H. Ashrafian, T. Athanasiou, Z. Takats, D. J. Hadjiminas, A. Darzi, and D. R. Leff, "Diagnostic accuracy of intraoperative techniques for margin assessment in breast cancer surgery," Ann. Surg. **265**(2), 300–310 (2017).
16. L. De Boer, B. Molenkamp, T. Bydlon, B. Hendriks, J. Wesseling, H. Sterenborg, and T. J. Ruers, "Fat/water ratios measured with diffuse reflectance spectroscopy to detect breast tumor boundaries," Breast Cancer Res. Treat. **152**(3), 509–518 (2015).
17. D. J. Evers, R. Nachabe, M.-J. V. Peeters, J. A. van der Hage, H. S. Oldenburg, E. J. Rutgers, G. W. Lucassen, B. H. Hendriks, J. Wesseling, and T. J. Ruers, "Diffuse reflectance spectroscopy: towards clinical application in breast cancer," Breast Cancer Res. Treat. **137**(1), 155–165 (2013).
18. L. L. de Boer, E. Kho, F. van Duijnhoven, M.-J. T. V. Peeters, K. K. Van de Vijver, B. H. Hendriks, H. J. Sterenborg, and T. J. Ruers, "Towards detection of positive resection margins with diffuse reflectance spectroscopy during breast conserving surgery (Conference Presentation)," in *Diseases in the Breast and Reproductive System V*, (International Society for Optics and Photonics, 2019), 108560H.
19. L. L. De Boer, T. M. Bydlon, F. Van Duijnhoven, M.-J. T. V. Peeters, C. E. Loo, G. A. Winter-Warnars, J. Sanders, H. J. Sterenborg, B. H. Hendriks, and T. J. Ruers, "Towards the use of diffuse reflectance spectroscopy for real-time in vivo detection of breast cancer during surgery," J. Transl. Med. **16**(1), 367 (2018).
20. R. Nachabé, B. H. Hendriks, G. W. Lucassen, M. van der Voort, D. J. Evers, E. J. Rutgers, M.-J. V. Peeters, J. A. Van der Hage, H. S. Oldenburg, and T. J. Ruers, "Diagnosis of breast cancer using diffuse optical spectroscopy from 500 to 1600 nm: comparison of classification methods," J. Biomed. Opt. **16**(8), 087010 (2011).
21. J. W. Spliethoff, W. Prevoo, M. A. Meier, J. de Jong, H. M. Klomp, D. J. Evers, H. J. Sterenborg, G. W. Lucassen, B. H. Hendriks, and T. J. Ruers, "Real-time in vivo tissue characterization with diffuse reflectance spectroscopy during transthoracic lung biopsy: a clinical feasibility study," Clin. Cancer Res. **22**(2), 357–365 (2016).
22. L. L. de Boer, B. H. Hendriks, F. Van Duijnhoven, M.-J. T. V. Peeters-Baas, K. Van de Vijver, C. E. Loo, K. Jóźwiak, H. J. Sterenborg, and T. J. Ruers, "Using DRS during breast conserving surgery: identifying robust optical parameters and influence of inter-patient variation," Biomed. Opt. Express **7**(12), 5188–5200 (2016).
23. D. J. Evers, A. C. Westerkamp, J. W. Spliethoff, V. V. Pully, D. Hompes, B. H. Hendriks, W. Prevoo, M. L. F. van Velthuysen, R. J. Porte, and T. J. Ruers, "Diffuse reflectance spectroscopy: toward real-time quantification of steatosis in liver," Transplant Int. **28**(4), 465–474 (2015).
24. E. J. Baltussen, P. Snæbjörnsson, S. G. B. De Koning, H. J. Sterenborg, A. G. Aalbers, N. Kok, G. L. Beets, B. H. Hendriks, K. F. Kuhlmann, and T. J. Ruers, "Diffuse reflectance spectroscopy as a tool for real-time tissue assessment during colorectal cancer surgery," J. Biomed. Opt. **22**(10), 1 (2017).
25. M. Jermyn, J. Mercier, K. Aubertin, J. Desroches, K. Urmey, J. Karamchandiani, E. Marple, M.-C. Guiot, F. Leblond, and K. Petrecca, "Highly accurate detection of cancer in situ with intraoperative, label-free, multimodal optical spectroscopy," Cancer Res. **77**(14), 3942–3950 (2017).
26. A. Taheri, P. Mansoori, L. F. Sandoval, S. R. Feldman, D. Pearce, and P. M. Williford, "Electrosurgery: part II. Technology, applications, and safety of electrosurgical devices," J. Am. Acad. Dermatol. **70**(4), 607.e1–607.e12 (2014).
27. A. Yaroslavsky, P. Schulze, I. Yaroslavsky, R. Schober, F. Ulrich, and H. Schwarzmaier, "Optical properties of selected native and coagulated human brain tissues in vitro in the visible and near infrared spectral range," Phys. Med. Biol. **47**(12), 3052059–2073 (2002).
28. G. J. Derbyshire, D. K. Bogen, and M. Unger, "Thermally induced optical property changes in myocardium at 1.06 μm," Lasers Surg. Med. **10**(1), 28–34 (1990).
29. J. P. Ritz, A. Roggan, C. Isbert, G. Müller, H. J. Buhr, and C. T. Germer, "Optical properties of native and coagulated porcine liver tissue between 400 and 2400 nm," Lasers Surg. Med. **29**(3), 205–212 (2001).
30. R. Nachabé, B. H. Hendriks, M. van der Voort, A. E. Desjardins, and H. J. Sterenborg, "Estimation of biological chromophores using diffuse optical spectroscopy: benefit of extending the UV-VIS wavelength range to include 1000 to 1600 nm," Biomed. Opt. Express **1**(5), 1432–1442 (2010).
31. R. Nachabe, B. H. Hendriks, A. E. Desjardins, M. van der Voort, M. B. van der Mark, and H. J. J. J. o. b. o. Sterenborg, "Estimation of lipid and water concentrations in scattering media with diffuse optical spectroscopy from 900 to 1600 nm," J. Biomed. Opt. **15**(3), 037015 (2010).
32. C. A. Schneider, W. S. Rasband, and K. W. Eliceiri, "NIH Image to ImageJ: 25 years of image analysis," Nat. Methods **9**(7), 671–675 (2012).
33. J. I. Goldstein, D. E. Newbury, J. R. Michael, N. W. Ritchie, J. H. J. Scott, and D. C. Joy, *Scanning Electron Microscopy and X-ray Microanalysis* (Springer, 2017).
34. G. A. Vilos and C. Rajakumar, "Electrosurgical generators and monopolar and bipolar electrosurgery," J Minim Invasive Gynecol **20**(3), 279–287 (2013).
35. M. G. Munro, "Fundamentals of electrosurgery part I: principles of radiofrequency energy for surgery," in *The SAGES Manual on the Fundamental Use of Surgical Energy (FUSE)* (Springer, 2012), pp. 15–59.
36. M. Annals of surgeryRedígolo, R. Aguiar, C. Zamboni, and I. Sato, "Determination of reference interval values for inorganic elements in whole blood samples of humans and laboratory animals by X-ray fluorescence spectrometry," J. Radioanal. Nucl. Chem. **297**(3), 463–467 (2013).

Biomedical Optics EXPRESS

37. T. M. Bydlon, R. Nachabé, N. Ramanujam, H. J. Sterenborg, and B. H. Hendriks, "Chromophore based analyses of steady-state diffuse reflectance spectroscopy: current status and perspectives for clinical adoption," J. Biophotonics **8**(1-2), 9–24 (2015).
38. S. C. Feng, F. Zeng, and B. Chance, "Monte Carlo simulations of photon migration path distributions in multiple scattering media," in *Photon Migration and Imaging in Random Media and Tissues*, (International Society for Optics and Photonics, 1993), 78–89.
39. A. Koenig, B. Roig, J. Le Digabel, G. Josse, and J.-M. Dinten, "Accessing deep optical properties of skin using diffuse reflectance spectroscopy," in *European Conference on Biomedical Optics*, (Optical Society of America, 2015), 95370E.
40. J. W. Spliethoff, E. Tanis, D. J. Evers, B. H. Hendriks, W. Prevoo, and T. J. Ruers, "Monitoring of tumor radio frequency ablation using derivative spectroscopy," J. Biomed. Opt. **19**(9), 097004 (2014).